synthesized and characterized. These are the first examples that contain phosphite ligands. The larger triisopropyl phosphite ligand gave clusters with $y = 4$ and 5 while, with the smaller trimethyl phosphite ligand, clusters with $y = 5$ and 6 were formed. This is an expected trend based on steric crowding around the rhodium atom. The hydride ligands in these clusters are thought to be bridging the Ru–Au bonds. Although these compounds are unreactive toward small molecules such as CO, PPh_3, and H_2 and have not shown catalytic reactivity, they do serve to broaden the range of metal–gold cluster compounds. Work is continuing on these and related clusters in an effort to understand the factors that determine their novel structures.

Acknowledgment. This work was supported by the National Science Foundation (Grant NSF CHE-8818187) and the donors of the Petroleum Research Fund, administered by the American Chemical Society.

Supplementary Material Available: Figure S1, displaying the ORTEP drawing of **1**, Figure S2, showing the positive ion FABMS of **3**, Table S1, listing the complete crystal data and data collection parameters, and Tables S2–S6, listing general temperature factor expressions, final positional and thermal parameters for all atoms including solvate molecules, distances and angles, and least-squares planes (15 pages); Table S7, listing observed and calculated structure factor amplitudes (33 pages). Ordering information is given on any current masthead page.

Contribution from the Corporate Research Science Laboratories, Exxon Research and Engineering Company, Annandale, New Jersey 08801, and Department of Chemistry, University of California at Berkeley, and Materials and Chemical Sciences Division, Lawrence Berkeley Laboratory, Berkeley, California 94720

Models for Organometallic Polymers. Zigzag Chains of $Mo_2(O_2CCH_3)_4$ Units Linked by DMPE and TMED Ligands

Michael C. Kerby,*,† Bryan W. Eichhorn,*,‡ J. Alan Creighton,§ and K. Peter C. Vollhardt∥

Received April 28, 1989

Infinite zigzag chains of $Mo_2(O_2CCH_3)_4$ units linked by the bidentate ligands 1,2-bis(dimethylphosphino)ethane (dmpe) and tetramethylethylenediamine (tmed) crystallize from solutions of $Mo_2(O_2CCH_3)_4$ (**1**) dissolved in the respective *neat* ligand. Single-crystal X-ray structures of the light yellow polymers $^1_\infty[Mo_2(O_2CCH_3)_4(dmpe)]$ (**2**) and $^1_\infty[Mo_2(O_2CCH_3)_4(tmed)]$ (**3**) showed that the compounds were isostructural. Compound **2** crystallizes in space group $P\bar{1}$ (−135 °C) with $a = 8.473$ (2) Å, $b = 9.562$ (3) Å, $c = 7.654$ (3) Å, $\alpha = 110.59$ (2)°, $\beta = 100.06$ (2)°, $\gamma = 69.26$ (2)°, $Z = 1$, $V = 541.9$ (3) Å^3, $R = 0.058$, and $R_w = 0.058$. Compound **3** crystallizes in space group $P\bar{1}$ (20 °C) with $a = 8.388$ (1) Å, $b = 8.445$ (2) Å, $c = 8.840$ (2) Å, $\alpha = 105.95$ (2)°, $\beta = 115.62$ (1)°, $\gamma = 91.63$ (2)°, $Z = 1$, $V = 535.1$ (2) Å^3, $R = 0.025$, and $R_w = 0.033$. The ligands dmpe and tmed are coordinated axially through weak Mo–L bonds to relatively unperturbed $Mo_2(O_2CCH_3)_4$ centers. The solid-state Raman spectrum of **3** reveals a small decrease in the Mo–Mo stretching frequency ($\nu_{Mo-Mo} = 391$ cm^{-1}) relative to **1** ($\nu_{Mo-Mo} = 405$ cm^{-1}). TGA and powder X-ray diffraction studies involving **3** showed that solid-state thermolysis results in the expulsion of tmed at 92 °C and the formation of crystalline **1**.

Introduction

Interest in low-dimensional metal-containing polymers has been stimulated because of their potential to have the electrical and optical properties found in metals.[1] A severe impediment to the formation of oligomers from dinuclear metal complexes is the propensity of the latter to condense into metal clusters.[2] However, several bimetallic carboxylates, $M_2(O_2CR)_4$,[3] produce such polymers when treated with coordinating bidentate bases. For example, the addition of pyrazine (pyz) to aqueous solutions of dicopper(II) tetraacetate furnishes linear arrays of $Cu_2(O_2CCH_3)_4(pyz)$ units.[4] Similarly, an isomorphous pyrazine adduct of dichromium(II) tetraacetate was structurally characterized, revealing one-dimensional chains comprising $Cr_2(O_2CCH_3)_4(pyz)$ fragments.[5] Linear and zigzag chains of dirhodium(II) tetracarboxylates are produced with the bidentate ligands phenazine and durenediamine, respectively.[6] Recently, the structure of $Cu_2L_2(O_2CCH_3)_2 \cdot Cu_2(O_2CCH_3)_4 \cdot 2EtOH$ [where LH = *N*-methyl-*N'*-(4,6-dimethoxysalicylidene)-1,3-propanediamine] was reported in which alternating dicopper(II) subunits are linked through hydrogen bonds to form a one-dimensional array.[7] We were interested in assessing the effects of hydrogen bonding and ligand polarity in the synthesis of related one-dimensional compounds containing $Mo_2(O_2CCH_3)_4$ subunits.

Tertiary phosphines react with $M_2(O_2CCF_3)_4$ (M = Mo, W) to produce two classes of Lewis base adducts shown by I and II.[8-13]

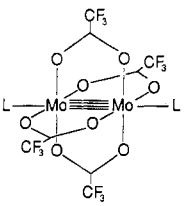

I

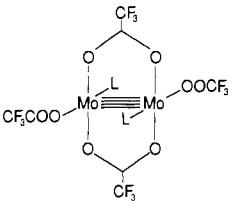

II

The preference for a particular structure type can be predicted rather well by analysis of phosphine cone angle and basicity values of the phosphine ligands. Spectroscopic studies have shown that the addition of bulky tertiary phosphines [i.e. $PMePh_2$, PPh_3,

† Exxon Research and Engineering Co. Present address: Exxon Research and Development Laboratories, P.O. Box 2226, Baton Rouge, LA 70821.
‡ Exxon Research and Engineering Co. Present address: Department of Chemistry and Biochemistry, University of Maryland, College Park, MD 20742.
§ Exxon Research and Engineering Co. Present address: Chemical Laboratories, University of Kent, Canterbury CT2 7NH, U.K.
∥ UC Berkeley.

(1) Miller, J. S. *Extended Linear Chain Compounds*; Plenum Press: New York, 1981–83; Vols. 1–3.
(2) Gates, B. C., Guczi, L., Knozinger, H., Eds. *Metal Clusters in Catalysis*; Elsevier: Amsterdam, 1986.
(3) Cotton, F. A.; Walton, R. A. *Multiple Bonds Between Metal Atoms*; John Wiley & Sons: New York, 1982.
(4) (a) Valentine, J. S.; Silverstein, A. J.; Soos, Z. G. *J. Am. Chem. Soc.* **1974**, *96*, 97. (b) Morosin, B.; Hughes, R. C.; Soos, Z. G. *Acta Crystallogr., Sect. B: Struct. Crystallogr. Cryst. Chem.* **1975**, *B31*, 762.
(5) Cotton, F. A.; Felthouse, T. R. *Inorg. Chem.* **1980**, *19*, 328.
(6) Cotton, F. A.; Felthouse, T. R. *Inorg. Chem.* **1981**, *20*, 600.
(7) Chiari, B.; Piovesana, O.; Tarantelli, T.; Zanazzi, P. F. *Inorg. Chem.* **1988**, *27*, 3246.
(8) Girolami, G. S.; Mainz, V. V.; Andersen, R. A. *Inorg. Chem.* **1980**, *19*, 805.
(9) Santure, D. J.; McLaughlin, K. W.; Huffman, J. C.; Sattelberger, A. P. *Inorg. Chem.* **1983**, *22*, 1877.
(10) Girolami, G. S.; Andersen, R. A. *Inorg. Chem.* **1982**, *21*, 1318.
(11) Cotton, F. A.; Lay, D. G. *Inorg. Chem.* **1981**, *20*, 935. With the ligand PPh_2Me, both class I and class II complexes are isolated; see this reference and ref 10.
(12) Hursthouse, M. B.; Malik, K. M. *Acta Crystallogr., Sect. B* **1979**, *B35*, 2709.
(13) Santure, D. J.; Sattelberger, A. P. *Inorg. Chem.* **1985**, *24*, 3477.

0020-1669/90/1329-1319$02.50/0

$P(c\text{-}Hx)_3$, $P(t\text{-}Bu)_3$, $P(SiMe_3)_3$] to the trifluoroacetate complex, $Mo_2(O_2CCF_3)_4$, yields class I complexes containing axially coordinated phosphine ligands.[8,10] Typically, these systems exhibit long metal–phosphorus bond distances (>2.96 Å), which reflect weak metal–ligand interactions. The addition of less sterically hindered phosphines [i.e. PMe_3, PEt_3, $P(n\text{-}Bu)_3$, PMe_2Ph, $PMePh_2$, PEt_2Ph] yields class II complexes in which the equatorial phosphines bind trans to the resultant monodentate acetate groups. Typical Mo–P bond distances for class II complexes are considerably shorter (i.e. 2.51–2.54 Å).[11-13]

Other structurally characterized Lewis base adducts with class I type geometries include the diethylene glycol dimethyl ether (diglyme) complex $Mo_2(O_2CC_6H_5)_4(diglyme)_2$[14] and the pyridine complex $Mo_2(O_2CCF_3)_4(py)_2$.[15] However, to the best of our knowledge, examples of structurally characterized class I type systems derived from the parent tetraacetate dimer, $Mo_2(O_2CCH_3)_4$ (**1**), were unknown prior to these studies. This paper describes the first representatives of zigzag chains containing the dimolybdenum tetraacetate complex, **1**, bridged by the bidentate ligands bis(dimethylphosphino)ethane (dmpe) and tetramethylethylenediamine (tmed). The structures of these compounds reveal the diaxial coordination of the bidentate ligands that link independent $Mo_2(O_2CCH_3)_4$ units into weakly associated one-dimensional polymers.

Experimental Section

All reactions were performed under dry argon in a Vacuum Atmospheres glovebox equipped with a HE-493 dri-train. 1,2-Bis(dimethylphosphino)ethane (dmpe) was purchased from Strem Chemicals and used as received. Tetramethylethylenediamine (tmed) was purchased from Aldrich Chemical Co., distilled twice from sodium under argon, and stored over 3-Å molecular sieves. Hexanes were distilled from sodium under nitrogen and stored over 3-Å molecular sieves. Dimolybdenum tetraacetate, $Mo_2(O_2CCH_3)_4$, was synthesized as described previously.[16]

Infrared spectra were recorded on an IBM 32 FTIR spectrometer from KI pellets pressed in the glovebox. TGA data were collected on a Du Pont 951 thermogravimetric analyzer coupled with a Du Pont 1090 data analysis station. The samples were run under a He purge at a heating rate of 10 °C/min. The powder X-ray diffraction data were collected by using an airtight beryllium-windowed cell on a Phillips XRG-3000 powder diffractometer. The residues in the TGA experiments were identified by comparing their powder X-ray diffraction patterns with that of authentic $Mo_2(O_2CCH_3)_4$. Raman spectra were measured on a Spex Triplemate spectrometer with a Spectra-Physics Kr laser (6471-Å exciting radiation). Crushed samples were added to glass capillaries and sealed under argon. Mass spectral data were recorded on a Finnigan 4500 mass spectrometer using a direct insertion probe. Elemental analyses were performed by Schwarzkopf Microanalytical Laboratory, Woodside, New York. Crystallographic services were provided by Dr. J. D. Ferrara of the Molecular Structure Co., College Station, TX, and Dr. Cynthia S. Day of Crystalytics Co., Lincoln, NE.

Synthesis of $^1_\infty$[$Mo_2(O_2CCH_3)_4$(dmpe)] (2). In the glovebox, a vial containing $Mo_2(O_2CCH_3)_4$ (67 mg, 0.16 mmol) and dmpe (2.0 g, 13 mmol) was heated to 130 °C. The color of the solution gradually changed from colorless to pink, then orange, then red, and finally purple as the $Mo_2(O_2CCH_3)_4$ slowly dissolved. After 2 h at 130 °C, the mixture was cooled slowly (over a 2-h period) to 30 °C. The reaction mixture was filtered several times to remove unreacted $Mo_2(O_2CCH_3)_4$ (recovered 24 mg, 0.06 mmol). The volume of the filtrate was reduced in vacuo by approximately 50%. After several days, pale yellow crystals of **2** were collected by filtration, washed with hexane (2 × 10 mL), and dried in vacuo (6 mg, 10% yield); mp 182–186 °C dec. IR (KI, cm^{-1}): ν_{OCO} = 1534 (s), 1430 (s, br). MS (CI): m/e 578 (M^+). Anal. Calcd for $C_{14}H_{28}O_8P_2Mo_2$: C, 29.08; H, 4.88. Found: C, 27.24; H, 3.85.

Synthesis of $^1_\infty$[$Mo_2(O_2CCH_3)_4$(tmed)] (3). To a vial in the glovebox was added $Mo_2(O_2CCH_3)_4$ (116 mg, 0.27 mmol) and dry tmed (10 mL). The mixture was warmed to 100 °C for 1 h, resulting in a clear yellow solution, which was slowly cooled to 30 °C. After 12 h, pale yellow crystals of **3** were collected by filtration, washed with hexane (2 × 10 mL), and dried in vacuo (124 mg, 84%); mp 123–127 °C dec. IR (KI, cm^{-1}): ν_{OCO} = 1526 (s), 1431 (s, br). MS (CI): m/e 428 (M^+ – tmed), 116 (tmed). Anal. Calcd for $C_{14}H_{28}O_8N_2Mo_2$: C, 30.90; H, 5.19; N, 5.15. Found: C, 31.16; H, 5.39; N, 5.59.

Table I. Crystallographic Data for **2** and **3**

	2	**3**
chem formula	$C_{14}H_{28}O_8P_2Mo_2$	$C_{14}H_{28}O_8N_2Mo_2$
space group	$P\bar{1}$ (No. 2)	$P\bar{1}$ (No. 2)
fw	578.20	544.26
a, Å	8.473 (2)	8.388 (1)
b, Å	9.562 (3)	8.445 (2)
c, Å	7.654 (3)	8.840 (2)
α, deg	110.59 (2)	105.95 (2)
β, deg	100.06 (2)	115.62 (1)
γ, deg	69.26 (2)	91.63 (2)
V, Å^3	541.9 (3)	535.1 (2)
Z	1	1
T, °C	−135	+20
λ, Å	0.7107	0.7107
ρ_{calcd}, g cm^{-3}	1.771	1.690
μ, cm^{-1}	13.09	11.8
R	0.058	0.025
R_w	0.058	0.033

X-ray Structure Determinations. $^1_\infty$[$Mo_2(O_2CCH_3)_4$(dmpe)] (2). A summary of the crystal data is given in Table I. A yellow, lump-shaped crystal was mounted on a glass fiber. Twenty reflections in the range 13.75° < 2θ < 25.45° were used to index and refine the unit cell (triclinic) and establish an orientation matrix for data collection.

Data were collected by using an ω–2θ scan technique. Three intensity and orientation check reflections were measured after every 150 reflections and did not vary during the course of data collection. The data were corrected for Lorentz and polarization effects, and an empirical absorption was applied. The molybdenum atom was located by direct methods (SHELXS-86), and the remainder of the structure was solved and refined by a combination of difference Fourier syntheses and least-squares refinements. All non-hydrogen atoms were refined anisotropically, and the hydrogen atoms were placed in idealized positions and included in the structure factor calculation as fixed-atom contributors (d_{C-H} = 0.95 Å) in the final cycles of refinement. The final difference Fourier map was essentially featureless.

$^1_\infty$[$Mo_2(O_2CCH_3)_4$(tmed)] (3). A summary of the crystal data is given in Table I. A yellow, rectangular parallelepiped crystal was sealed inside a glass capillary under N_2. Fifteen computer-centered reflections with 2θ > 25° were used to index and refine the unit cell (triclinic).

Data were collected by using an ω-scan technique with a 1.0° scan range and corrected for Lorentz and polarization effects. Absorption corrections were not necessary and not applied. The molybdenum atom was located by heavy-atom Patterson techniques, and the remainder of the structure was solved and refined by a combination of least-squares refinements and difference Fourier syntheses. All non-hydrogen atoms were refined anistropically. The four methyl groups [C(2), C(4), C(6), C(7)] were refined as rigid rotors with sp^3-hybridized geometry and a C–H bond length of 0.96 Å. The final orientation of each methyl group was determined by three rotational parameters. The remaining hydrogen atoms were included in the structure factor calculation as idealized atoms and were assigned isotropic thermal parameters. The final difference Fourier map contained two peaks above background, which were within 1.05 Å of a molybdenum atom.

Results and Discussion

Preparation and Characterization of $^1_\infty$[$Mo_2(O_2CCH_3)_4$(dmpe)] (2). Yellow, crystalline $Mo_2(O_2CCH_3)_4$ (**1**) slowly dissolves in dmpe, forming a faint pink solution after several hours at room temperature. Upon warming to 130 °C for several hours, the solution changes in color from pink to orange, to red, and, finally, to purple. The solution retains its purple color upon cooling. After several days at room temperature, X-ray-quality, light yellow crystals of **2** can be isolated from the purple solution in low yield (eq 1).

$$Mo_2(O_2CCH_3)_4 \xrightarrow[130°C]{dmpe} \underset{2}{^1_\infty [Mo_2(O_2CCH_3)_4(dmpe)]} \quad (1)$$

EDAX analysis of the crystals revealed a 1:1 ratio of Mo to P. The compound is indefinitely stable under argon, but darkens to a brown color after several hours in air. Although **2** is insoluble in most organic solvents, it can be redissolved in neat dmpe, producing pink-red solutions. The solid-state infrared spectrum

(14) Collins, D. M.; Cotton, F. A.; Murillo, C. A. *Inorg. Chem.* **1976**, *15*, 2950.
(15) Cotton, F. A.; Norman, J. G., Jr. *J. Am. Chem. Soc.* **1972**, *94*, 5697.
(16) Stephenson, T. A.; Bannister, E.; Wilkinson, G. *J. Chem. Soc.* **1964**, 2538.

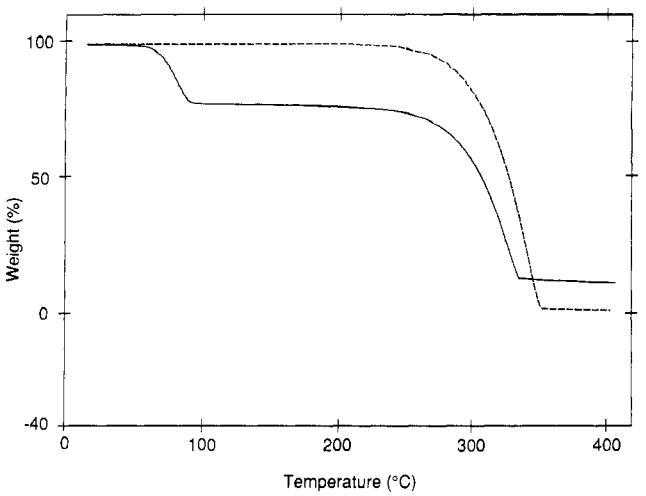

Figure 1. Plot of percent weight loss versus temperature for the thermal decomposition of **3** (solid line) and $Mo_2(O_2CCH_3)_4$ (dotted line). The experiment was run in a He purge.

(KI pellet) of the crystalline solid exhibits asymmetric and symmetric acetate carbonyl stretching frequencies at 1534 (s) and 1430 (s) cm^{-1}, respectively, similar in energy to those found for **1**. Girolami and Andersen reported that an excess of dmpe (5.6 equiv) in an Et_2O solution of $Mo_2(O_2CCF_3)_4$ generated a complex mixture of orange mono-, blue di-, and pink-purple trisubstituted dmpe complexes bearing monodentate acetate ligands.[8,17] It is reasonable to infer that the color changes observed during the formation of **2** are due to the presence of soluble, substituted $Mo_2(O_2CCH_3)_4(dmpe)_x$ (x = 1–3) class II type complexes.

Preparation and Characterization of $^1_\infty$[$Mo_2(O_2CCH_3)_4$(tmed)] (3). The bis(amine) polymer (**3**) is prepared by the addition of **1** to neat tmed. The dramatic color changes that occurred during the dmpe reaction are not observed in the present system. Instead, a clear yellow solution is obtained after warming the mixture to 100 °C for 1 h. Upon slow cooling, large, light yellow single crystals of **3** are formed in yields ranging 80–90% (eq 2).

$$Mo_2(O_2CCH_3)_4 \xrightarrow[100°C]{\text{tmed}} {}^1_\infty[Mo_2(O_2CCH_3)_4(\text{tmed})] \quad (2)$$

3

The compound is insoluble in hexane, toluene, or THF but can be redissolved in warm tmed, producing clear yellow solutions. Compound **3** is more robust than its dmpe congener **2**, although crystalline samples will discolor from yellow to brown when exposed to air for several days. Previous studies have shown that similar synthetic procedures using neat pyridine yielded the nonpolymeric pyridine adducts $Mo_2(O_2CCH_3)_4(py)_2$[16] and $Mo_2(O_2CCF_3)_4(py)_2$.[15]

The solid-state IR spectrum of **3** (KI pellet) exhibits the characteristic asymmetric and symmetric acetate bands at 1526 (s) and 1431 (s, br) cm^{-1}, respectively, which are similar in energy to those of the parent compound **1**. TGA studies (Figure 1) reveal the thermal instability of **3** in that the tmed ligand (21% of compound mass) is expelled at 92 °C, producing a crystalline $Mo_2(O_2CCH_3)_4$ residue (powder X-ray diffraction). Further heating results in the sublimation of the resulting $Mo_2(O_2CCH_3)_4$. The TGA trace for an authentic sample of $Mo_2(O_2CCH_3)_4$ is also shown in Figure 1 (dashed line) for comparison.

Solid-State Structure of $^1_\infty$[$Mo_2(O_2CCH_3)_4$(dmpe)] (2). A CHEM-X[18] ball-and-stick representation of the dimolybdenum–dmpe complex **2** is shown in Figure 2. A summary of the crystal data is given in Table I. Fractional coordinates and selected bond distances and angles are presented in Tables II and III, respectively.

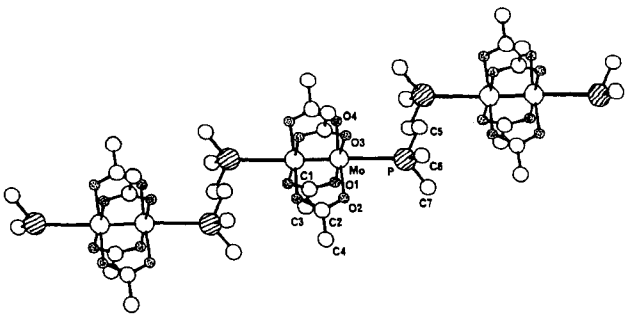

Figure 2. CHEM-X[18] representation of **2**. Unlabeled atoms are related by the inversion centers (i.e. midpoint of Mo–Mo bond and C–C bond in the ligand backbone).

Table II. Fractional Coordinates and Isotropic Thermal Parameters ($Å^2$) for **2**

	x	y	z	B_{iso}
Mo(1)	0.0737 (2)	0.3971 (2)	0.0333 (2)	1.22 (6)
P(1)	0.2703 (5)	0.1103 (4)	0.1633 (6)	2.3 (2)
O(1)	0.163 (1)	0.530 (1)	0.294 (1)	2.0 (5)
O(2)	0.002 (1)	0.749 (1)	0.225 (1)	2.1 (5)
O(3)	0.286 (1)	0.380 (1)	−0.090 (1)	2.3 (5)
O(4)	0.134 (1)	0.597 (1)	−0.162 (1)	1.9 (5)
C(1)	0.104 (2)	0.677 (2)	0.330 (2)	1.9 (7)
C(2)	0.168 (2)	0.775 (2)	0.515 (2)	3.1 (9)
C(3)	0.270 (2)	0.486 (2)	−0.161 (2)	2.2 (8)
C(4)	0.422 (2)	0.485 (2)	−0.244 (2)	3.1 (9)
C(5)	0.493 (2)	0.034 (2)	0.107 (2)	3.0 (8)
C(6)	0.220 (3)	−0.069 (2)	0.109 (3)	5 (1)
C(7)	0.293 (2)	0.164 (3)	0.415 (3)	6 (1)

Table III. Selected Bond Distances (Å) and Angles (deg) for **2**

Bond Distances			
Mo–Mo′	2.105 (3)	O(3)–C(3)	1.27 (2)
Mo–O(1)	2.12 (1)	O(4)–C(3)	1.27 (2)
Mo′–O(2)	2.13 (1)	C(3)–C(4)	1.53 (2)
Mo–O(3)	2.10 (1)	Mo–P	3.064 (4)
Mo′–O(4)	2.14 (1)	P–C(5)	1.83 (2)
O(1)–C(1)	1.26 (2)	P–C(6)	1.80 (2)
O(2)–C(1)	1.26 (2)	P–C(7)	1.80 (2)
C(1)–C(2)	1.53 (2)	C(5)–C(5′)	1.54 (3)
Bond Angles			
O(1)–Mo–Mo′	91.9 (3)	C(5)–P–C(6)	101.6 (8)
O(2)–Mo–Mo′	91.6 (3)	C(5)–P–C(7)	100.5 (8)
O(3)–Mo–Mo′	92.5 (3)	P–C(5)–C(5′)	110 (1)
O(4)–Mo–Mo′	90.9 (3)	C(6)–P–Mo	127.7 (7)
O(1)–Mo–O(2)	176.3 (4)	C(7)–P–Mo	111.4 (7)
O(3)–Mo–O(4)	176.6 (4)	O(1)–C(1)–O(2)	126 (1)
P–Mo–Mo′	174.7 (1)	O(1)–C(1)–C(2)	116 (1)
P–Mo–O(1)	85.2 (3)	O(2)–C(1)–C(2)	118 (1)
P–Mo–O(2)	91.3 (3)	O(3)–C(3)–O(4)	123 (1)
P–Mo–O(3)	91.9 (3)	O(3)–C(3)–C(4)	120 (1)
P–Mo–O(4)	84.7 (3)	O(4)–C(3)–C(4)	117 (1)
C(5)–P–Mo	111.9 (5)		

The structure of **2** comprises an infinite array of $Mo_2(O_2CCH_3)_4$ units bridged by dmpe ligands. The midpoints of both the molybdenum–molybdenum bond and the C–C bond of the dmpe ethylene backbone occupy crystallographic centers of inversion. The $Mo_2(O_2CCH_3)_4$ units are relatively unperturbed with a Mo–Mo bond distance (2.105 (3) Å) similar to that in the parent complex **1** (2.0934 (8) Å).[19] The Mo–O bond lengths in **2** range from 2.10 (1) to 2.14 (1) Å (average 2.12 (3) Å), which are statistically equivalent to those in **1** (average 2.119 (5) Å). The two planes defined by the two respective sets of trans acetate groups (e.g. O1, O1′, O2, O2′, C1, C1′, C2, C2′) and the Mo–Mo′ vector are nearly perfect, the average mean deviation from planarity being 0.02 (2) Å. The dihedral angle defined by the two planes is 90.7 (2)°.

(17) The trifluoroacetate derivative $Mo_2(O_2CCF_3)_4$ is soluble in most common organic solvents; see ref 8.

(18) CHEM-X, developed and distributed by Chemical Design Ltd., Oxford, England.

(19) Cotton, F. A.; Mester, Z. C.; Webb, T. R. *Acta Crystallogr., Sect. B* **1974**, *B30*, 2768.

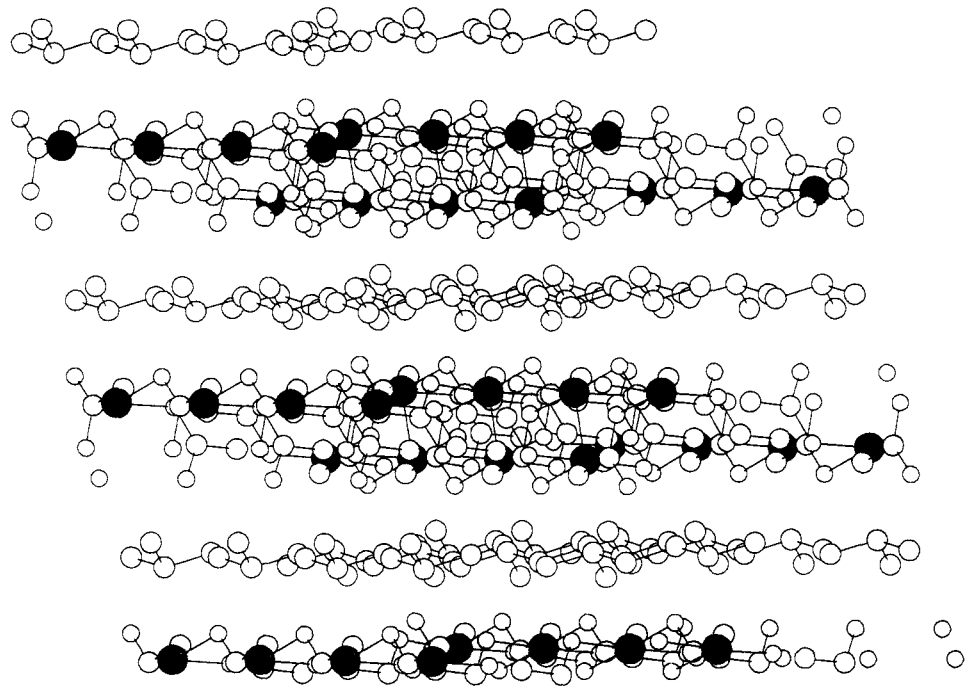

Figure 3. Ball-and-stick packing diagram of **3** (Mo–N bonds omitted), showing the sheets of isolated $Mo_2(O_2CCH_3)_4$ units separated by layers of tmed ligands. The filled balls represent Mo atoms. The drawing shows approximately 18 unit cells.

Table IV. Fractional Coordinates and Isotropic Thermal Parameters ($Å^2$) for **3**

	x	y	z	B_{iso}
Mo(1)	0.1043 (1)	0.0382 (1)	0.1304 (1)	2.4 (1)
N(1)	0.3307 (2)	0.1470 (2)	0.4851 (2)	3.0 (1)
O(1)	−0.0663 (2)	0.1630 (2)	0.2267 (2)	3.0 (1)
O(2)	−0.2860 (2)	0.0799 (2)	−0.0497 (2)	3.0 (1)
O(3)	0.0270 (2)	−0.1806 (2)	0.1726 (2)	3.2 (1)
O(4)	−0.1941 (2)	−0.2605 (2)	−0.1033 (2)	3.2 (1)
C(1)	−0.2276 (3)	0.1555 (2)	0.1144 (3)	2.8 (1)
C(2)	−0.3532 (3)	0.2370 (3)	0.1774 (4)	3.8 (1)
C(3)	−0.1079 (3)	−0.2832 (3)	0.0451 (3)	3.1 (1)
C(4)	−0.1694 (4)	−0.4380 (3)	0.0701 (4)	4.8 (1)
C(5)	0.5063 (3)	0.0946 (3)	0.5267 (3)	3.0 (1)
C(6)	0.2469 (4)	0.0951 (4)	0.5830 (4)	4.3 (1)
C(7)	0.3559 (4)	0.3287 (3)	0.5310 (4)	4.6 (1)

The terminal Mo–P contacts in **2** are very long (3.064 (4) Å) and are characteristic of the weak, axial interactions found in type I compounds. Monodentate phosphine adducts of the trifluoroacetate molybdenum dimer, $Mo_2(O_2CCF_3)_4(L)_2$, exhibit similar Mo–P bond distances of 2.988 (2) Å (L = $PMePh_2$)[10] and 3.07 (5) Å (L = PPh_3).[11] The Mo–Mo′–P bond angle in **2** (174.7 (1)°) is more linear than that in the trifluoroacetate–$PMePh_2$ complex, in which the average Mo–Mo–P bond angle is 166.15 (2)°.[10] The tetrahedral carbon and phosphorus atoms of the dmpe ligand impart a zigzag geometry on the one-dimensional chains [Mo1–P1–C5 = 111.9 (5)°, P1–C5–C5′ = 110 (1)°]. A similar structure was also observed in the dirhodium chain complex $^1_\infty[Rh_2(O_2CC_2H_5)_4(DDA)]$ (DDA = 2,3,5,6-tetramethyl-*p*-phenylenediamine), which contained a Rh–N–C bond angle of 118.8 (4)°.[6]

Surprisingly, the mass spectrum for **2** (chemical ionization) shows a peak corresponding to the parent ion $[Mo_2(O_2CCH_3)_4(dmpe)]^+$ despite the weak Mo–P interactions.

Solid-State Structure of $^1_\infty[Mo_2(O_2CCH_3)_4(tmed)]$ (3) and Bonding Considerations. Fractional coordinates and selected bond distances and angles for the dimolybdenum–tmed compound **3** are given in Tables IV and V, respectively. A summary of crystallographic data is presented in Table I. The complex also crystallizes as a weakly associated, one-dimensional polymer and is isostructural with **2** (see Figure 2). The midpoints of the molybdenum–molybdenum bond and the carbon–carbon bond in the tmed backbone are both located on crystallographic centers of inversion. As in **2**, the $Mo_2(O_2CCH_3)_4$ core in **3** is virtually unperturbed with a Mo–Mo bond distance of 2.103 (1) Å, just slightly longer than that in the parent complex **1** (2.0934 (8) Å).[19] Similarly, compound **3** also displays long, axial metal–ligand contacts that are virtually nonbonding. The Mo–N distances in **3** [2.729 (2) Å] are similar to the axial Mo–N contacts observed in the two dications $[Mo_2(O_2CCH_3)_2(H_2NCH_2CH_2NH_2)_4]^{2+}$ [2.77 (3) Å (average)][20] and $[Mo_2(O_2CCH_3)_2(CH_3CN)_6]^{2+}$ [2.64 (2) and 2.77 (2) Å].[21,22] The packing diagram of **3** with the Mo–N bonds omitted, shown in Figure 3, illustrates the separated sheets of isolated $Mo_2(O_2CCH_3)_4$ units that are spaced by layers of tmed ligands in the crystal lattice.

Mass spectroscopic experiments involving **3** (chemical ionization) show two major peaks corresponding to $Mo_2(O_2CCH_3)_4^+$

Table V. Selected Bond Distances (Å) and Angles (deg) for **3**

Bond Distances			
Mo–Mo′	2.103 (1)	O(3)–C(3)	1.268 (2)
Mo–O(1)	2.128 (2)	O(4)–C(3)	1.267 (3)
Mo′–O(2)	2.113 (2)	C(3)–C(4)	1.497 (4)
Mo–O(3)	2.119 (2)	Mo–N	2.729 (2)
Mo′–O(4)	2.115 (2)	N–C(5)	1.470 (3)
O(1)–C(1)	1.272 (2)	N–C(6)	1.467 (5)
O(2)–C(1)	1.269 (3)	N–C(7)	1.458 (3)
C(1)–C(2)	1.494 (4)	C(5)–C(5′)	1.523 (4)
Bond Angles			
O(1)–Mo–Mo′	91.0 (1)	C(5)–N–C(6)	110.8 (1)
O(2)–Mo–Mo′	92.3 (1)	C(5)–N–C(7)	103.8 (1)
O(3)–Mo–Mo′	91.4 (1)	C(5′)–C(5)–N	112.7 (2)
O(4)–Mo–Mo′	92.0 (1)	C(6)–N–Mo	110.8 (1)
O(1)–Mo–O(2)	176.7 (1)	C(7)–N–Mo	103.8 (1)
O(3)–Mo–O(4)	176.7 (1)	O(1)–C(1)–O(2)	122.2 (2)
N–Mo–Mo′	170.5 (1)	O(1)–C(1)–C(2)	119.1 (2)
N–Mo–O(1)	79.9 (1)	O(2)–C(1)–C(2)	118.7 (2)
N–Mo–O(2)	96.8 (1)	O(3)–C(3)–O(4)	122.8 (2)
N–Mo–O(3)	85.8 (1)	O(3)–C(3)–C(4)	120 (1)
N–Mo–O(4)	91.0 (1)	O(4)–C(3)–C(4)	117 (1)
C(5)–N–Mo	112.2 (1)		

(20) Eichhorn, B. W.; Kerby, M. C.; Haushalter, R. C.; Vollhardt, K. P. C. *Inorg. Chem.* **1990**, *29*, 723.
(21) Cotton, F. A.; Reid, A. H., Jr.; Schwotzer, W. *Inorg. Chem.* **1985**, *24*, 3965.
(22) A later structural determination of the same compound was reported to have Mo–N_{ax} contacts of 2.772 (8) and 2.745 (10) Å. See: Pimblett, G.; Garner, C. D.; Clegg, W. *J. Chem. Soc., Dalton Trans.* **1986**, 1257.

Table VI. Structural and Raman Spectral Data for Selected $Mo_2(O_2CCH_3)_4$ Complexes

	ν_{Mo-Mo}, cm^{-1}	Mo–L, Å	Mo–Mo, Å
$Mo_2(O_2CCH_3)_4$ (**1**)	406[a]		2.093 (2)
$Mo_2(O_2CCF_3)_4$	397[a]		2.090 (4)
$Mo_2(O_2CCH_3)_4(py)_2$	363[a]		
$Mo_2(O_2CCF_3)_4(py)_2$	367[a]	2.548 (8)	2.129 (2)
$Mo_2(O_2CCH_3)_4$ (**1**)	405[b]		2.093 (2)
$^1_\infty[Mo_2(O_2CCH_3)_4(tmed)]$ (**3**)	391[b]	2.729 (2)	2.103 (1)

[a] Raman spectra were determined with a Cary-81 spectrometer with a Spectra-Physics He–Ne laser (6328-Å exciting radiation); see ref 15. [b] Raman spectra were determined with a Spex Triplemate spectrometer with a Spectra-Physics Kr laser (6471-Å exciting radiation); this work.

and $tmed^+$, but the parent ion $[Mo_2(O_2CCH_3)_4(tmed)]^+$ is not observed. This behavior contrasts that observed for **2** and apparently reflects the weaker Lewis basicity of tmed relative to dmpe.

It has been suggested that the strong σ component found in Mo–Mo quadruple bonds ($\sigma^2\pi^4\delta^2$) precludes any low-lying acceptor orbitals for significant binding at axial positions.[15] Most axially coordinated $Mo_2(O_2CR)_4L_2$ complexes that have been structurally characterized all have long Mo–L contacts and Mo–Mo bond distances only slightly longer than those of the unligated parent compounds. Raman spectroscopy has been a useful spectroscopic tool for measuring metal–metal stretching frequencies (A_{1g} mode) and assessing M–M bond strength. Through this method, it was demonstrated that the A_{1g} band (ν_{Mo-Mo}) in $Mo_2(O_2CCF_3)_4$ decreased in energy as the donor ability of added axial ligands increased.[15] Similarly, the solid-state Raman spectra of the two py adducts, $Mo_2(O_2CR)_4(py)_2$ (R = CH_3, CF_3), show shifts in the A_{1g} band to lower energy relative to the parent complexes. Table VI lists solid-state ν_{Mo-Mo} values and Mo–Mo and Mo–L distances for selected $Mo_2(O_2CR)_4(L)_2$ complexes (R = CH_3, CF_3 and L = py) and for the tmed chain complex, **3**. Compared to the parent carboxylate, **1** (ν = 405 cm^{-1}), the tmed chain complex, **3**, exhibits only a slight decrease in ν_{Mo-Mo} (ν = 391 cm^{-1}; $\Delta\nu$ = 14 cm^{-1}) with respect to the py adduct compounds, $Mo_2(O_2CCH_3)_4(py)_2$ (ν = 363 cm^{-1}; $\Delta\nu$ = 43 cm^{-1}) and $Mo_2(O_2CCF_3)_4(py)_2$ (ν = 367 cm^{-1}; $\Delta\nu$ = 30 cm^{-1}). The combination of structural and Raman data points toward weaker axial Mo–N bonds for sp^3 nitrogen atoms of the tmed ligands relative to the sp^2 nitrogen atoms of pyridine.

Conclusion

One-dimensional, zigzag chains containing $Mo_2(O_2CCH_3)_4$ units linked by the bidentate ligands dmpe and tmed crystallize from solutions of $Mo_2(O_2CCH_3)_4$ dissolved in the appropriate ligand. These compounds of general formula $^1_\infty Mo_2(O_2CCH_3)_4(Me_2ECH_2CH_2EMe_2)]$ [where E = P (**2**), N (**3**)] have characteristically weak, axial Mo–L interactions but represent the first examples of one-dimensional chains comprising $Mo_2(O_2CCH_3)_4$ units. Not unexpectedly, the Mo–Mo stretching frequency, ν_{Mo-Mo}, of the tmed chain polymer exhibits only a slight shift to lower energy due to axial ligation. We have recently isolated a related one-dimensional chain complex of formula $^1_\infty[Mo_2(O_2CCH_3)_4(N,N'\text{-dmed})]$ (**4**) (where dmed = dimethylethylenediamine) containing $Mo_2(O_2CCH_3)_4$ units linked by *N,N'*-dmed ligands.[23] In contrast to the structures of **2** and **3**, that of compound **4** has a kinked-chain structure due to hydrogen bonding between the dmed amine hydrogens and the oxygen atoms of the coordinated acetate ligands.

Thermally, compound **3** expels tmed in the solid state at low temperatures (<100 °C), forming crystalline $Mo_2(O_2CCH_3)_4$. This weak interaction of the tmed ligand with the Mo_2 center is also evidenced by the absence of a parent ion in mass spectroscopic studies. Packing diagrams for **3** reveal an unusual arrangement of layers comprising sheets of isolated $Mo_2(O_2CCH_3)_4$ units separated by layers of tmed ligands. Thus, the formation and decomposition of **3** can be viewed as an intercalation–deintercalation process in which tmed is reversibly absorbed by $Mo_2(O_2CCH_3)_4$. In related studies, we have shown that 5 equiv of ethylenediamine (en) are expelled from the nonpolymeric complex $[Mo_2(O_2CCH_3)_2(en)_4][(O_2CCH_3)_2]\cdot en$ (**5**), which also yields crystalline $Mo_2(O_2CCH_3)_4$ upon decomposition. The latter reaction requires a migration of acetate ions in the solid state in contrast to the thermal decomposition of **3**.[20]

A primary goal of our research has focused on the use of neat ligands as solvents in an attempt to reversibly displace acetate groups from the $Mo_2(O_2CCH_3)_4$ complex and generate enhanced reactivity at the Mo_2^{4+} center. Not surprisingly, $Mo_2(O_2CCH_3)_4$ dissolved in tmed shows little reactivity toward external substrates such as alkynes or olefins. In contrast, $Mo_2(O_2CCH_3)_4$ dissolved in en readily reacts with terminal alkynes to produce isolable alkyne adducts.[24] Recent experiments involving *N,N*-dmed (versus *N,N'*-dmed) and methylethylenediamine (mmed) have yielded tetrameric compounds of formula $\{[Mo_2(O_2CMe)_3(Me_2NCH_2CH_2NH_2)_2][(O_2CMe)]\}_2$ and $\{[Mo_2(O_2CMe)_3(MeHNCH_2CH_2NH_2)_2][(O_2CMe)]\}_2\cdot x MeHNCH_2CH_2NH_2$ (where $x \leq 1$), respectively, both of which have one displaced acetate ligand per Mo_2 unit. Thus, as the polarity of the ligand increases, the number of displaced acetates increases (i.e. compound **5**) and the reactivity of the Mo_2^{4+} center is enhanced.

The present compounds, **2** and **3**, serve as models for one-dimensional materials in that they demonstrate the potential of linking specific molecular subunits together into an infinite array. The weak bonds joining the subunits together in these complexes preclude any one-dimensional properties; however, related dinuclear carboxylates containing strong axial M–L bonds [cf. $M_2(O_2CR)_4R'_2$ where M = Mo or W] could prove to be better precursors for new, low-dimensional materials.[25]

Acknowledgment. Exxon Research and Engineering Co. generously supported this research. K.P.C.V. is grateful for partial funding of this work by the Director, Office of Energy Research, Office of Basic Energy Sciences, Materials Science Division of the U.S. Department of Energy (Contract No. DE-AC03-76 SF 00098).

Supplementary Material Available: Tables of crystal and refinement data, coordinates and isotropic temperature factors for the hydrogen atoms, anisotropic thermal parameters for the non-hydrogen atoms, distances, angles, and least-squares planes and ORTEP diagrams of **2** and **3** (22 pages); a listing of observed and calculated structure factor amplitudes for both compounds (26 pages). Ordering information is given on any current masthead page.

(23) Eichhorn, B. W.; Kerby, M. C.; Vollhardt, K. P. C. Manuscript in preparation.

(24) Kerby, M. C.; Eichhorn, B. W.; Vollhardt, K. P. C. *J. Am. Chem. Soc.*, submitted for publication.

(25) Chisholm, M. H.; Clark, D. L.; Huffman, J. C.; Van Der Sluys, W. G.; Kober, E. M.; Lichtenberger, D. L.; Bursten, B. E. *J. Am. Chem. Soc.* **1987**, *109*, 6796.